Massive Star Formation: Observations Confront Theory
ASP Conference Series, Vol. 387, ©2008
H. Beuther, H. Linz, and Th. Henning, eds.

Infall and the Formation of a Massive Star

M. T. Beltrán

Universitat de Barcelona, Martí i Franquès 1, 08028 Barcelona, SPAIN

R. Cesaroni, L. Moscadelli, and L. Testi

Osservatorio Astrofisico di Arcetri-INAF, Largo E. Fermi 5, 50125 Firenze, ITALY

C. Codella

Istituto di Radioastronomia-INAF, Largo E. Fermi 5, 50125 Firenze, ITALY

R. S. Furuya

Subaru Telescope, 650 North Aohoku Place, Hilo, 96720 Hawaii, USA

C. Goddi

Harvard-Smithosnian Center for Astrophysics, 60 Garden St., Cambridge, MA 02138, USA

Abstract. We present evidence of infall in a circumstellar rotating toroid enshrouding a luminous star in the massive star-forming region G24.78+0.08. Besides being one of the rare direct detections of infall in a young high-mass star, our finding stands unique for the simultaneous presence of three elements in the same massive object: a rotating, collapsing toroid, a bipolar outflow, ejected along the rotation axis, and a hypercompact ionized HII region. The large accretion rate and the existence of a hypercompact HII region confirm that the accretion cannot be spherically symmetric and must occur in a circumstellar disk.

1. Introduction

High-mass star-forming regions host luminous far-infrared point sources, ultra-compact (UC) HII regions, and newly formed OB stars embedded in rich hot molecular cores that can be studied in a variety of tracers. H_2O, OH, and CH_3OH masers are also often observed close to typical signposts of massive star formation. With this in mind, Codella, Testi, & Cesaroni (1997) carried out an ammonia survey with the Medicina antenna towards a sample of H_2O and OH maser spots associated with infrared sources to assess the presence of molecular cores associated with the maser spots. The source G24.78+0.08 was among the strongest NH_3 emitters, and since then, it has been thoroughly observed in different tracers with single-dish telescopes and interferometers.

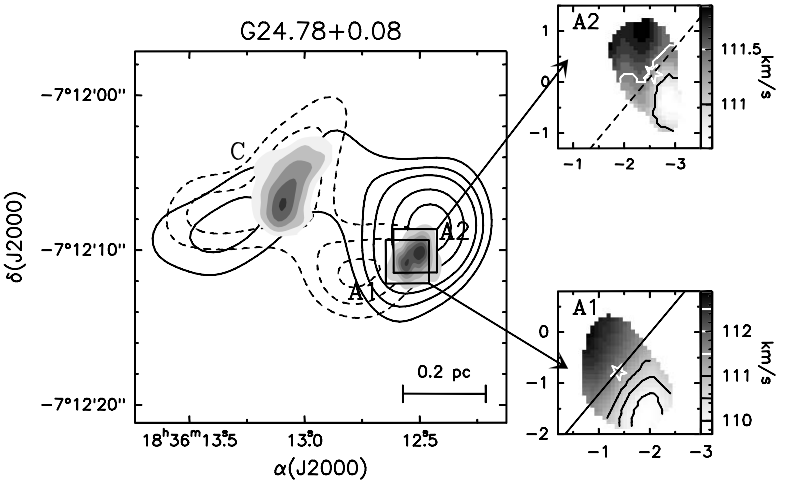

Figure 1. Comparison between the bipolar outflows observed by Furuya et al. (2002), the CH_3CN(12–11) line emission mapped by Beltrán et al. (2004) towards G24 A1 and G24 A2, and the CS(3–2) line map from Furuya et al. (2002) towards G24 C. The solid contours indicate blueshifted outflow emission and the dashed contours, redshifted one. On the right, map of the CH_3CN(12–11) line peak velocity towards G24 A2 and G24 A1 obtained with a Gaussian fit. The dashed and solid lines indicate the direction of the outflow. Figure adapted from Beltrán et al. (2004)

2. The high-mass star-forming region G24.78+0.08

G24.78+0.08 is a massive star-forming region located at a distance of 7.7 kpc that has a bolometric luminosity of $\leq 7\times10^4\ L_\odot$ and contains a cluster of massive young stellar objects, named A, B, C and D (Furuya et al. 2002) (see Fig. 1). Two of the molecular cores, cores A and B, are associated with ultracompact (UC) or hypercompact (HC) HII regions (Codella et al. 1997), and two of them, cores A and C, are associated with maser emission and are powering bipolar molecular outflows (Furuya et al. 2002). High-angular resolution observations of the continuum and the CH_3CN emission at 1 mm have resolved the core A into two separate cores, named A1 and A2 (Beltrán et al. 2004). The two cores are probably in a different evolutionary stage, as suggested by the fact that A1 is clearly associated with free-free emission at 1.3 cm while A2 is barely detected at 1.3 cm (see Fig. 2.). The emission of A1 is consistent with the star being a zero-age-main-sequence star of spectral type O9.5 (Codella et al. 1997), which corresponds to a mass of about 20 $M_\odot$. In addition, A2 has been clearly detected by Spitzer at 8 μm, while A1 was not detected.

By simultaneously fitting the multiple k-components of the different rotational transitions of CH_3CN(12-11), we discovered a clear velocity gradient towards both cores, orientated perpendicular to the axis of the molecular outflow (see Fig. 1; Beltrán et al. 2004; 2005). This suggests that CH_3CN is tracing rotation in these massive structures or toroids. These toroids are big and massive, with radii of ∼4000 AU and masses of 80 (A2) and 130 $M_\odot$ (A1), which are

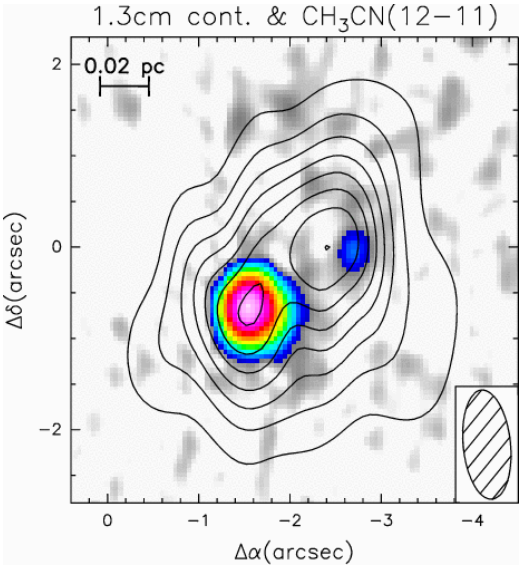

Figure 2. Map of the averaged CH_3CN(12-11) emission (*contours*) towards cores G24 A1 and G24 A2 (2004) and the 1.3 cm continuum emission of the HII regions (*grey scale*).

6 to 20 times larger than the dynamical masses needed for equilibrium. Hence, this suggests that the toroids might be unstable and undergoing collapse.

Recent CH_3OH maser emission observations have revealed two groups of masers associated with both cores A1 and A2, and aligned more or less perpendicular to the direction of the bipolar outflow (Moscadelli et al. 2007). Assuming that the mass inside the region traced by the maser emission (∼0.02 pc) is in rotational equilibrium, one derives a dynamical mass of 55 and 19 $M_\odot$ for G24 A1 and A2, respectively. For G24 A1, the dynamical mass is consistent with the mass of the central ionizing star, 20 $M_\odot$, plus the mass of the gas within 0.02 pc, which is ∼30 $M_\odot$.

3. The NH_3(2,2) emission

As the hypercompact HC HII region associated with G24 A1 is very bright at centimeter wavelengths (> 2000 K), it is very easy to observe the colder molecular gas (∼ 100 K) in absorption against it. We observed simultaneously the continuum emission and the ammonia NH_3(2,2) inversion transition at 1.3 cm wavelengths with the VLA in the B configuration. Figure 3 illustrates the most important finding of our study; that is, that the **toroid in G24 A1 is not only rotating, but also accreting onto the central star**.

As can be seen in the left panels of this figure, the line is seen in absorption towards the continuum of the HC HII region. In the top left panel, we show the map of the intensity integrated under the NH_3(2,2) inversion line (Beltrán et al. 2006). The black contours indicate emission, while the white contours

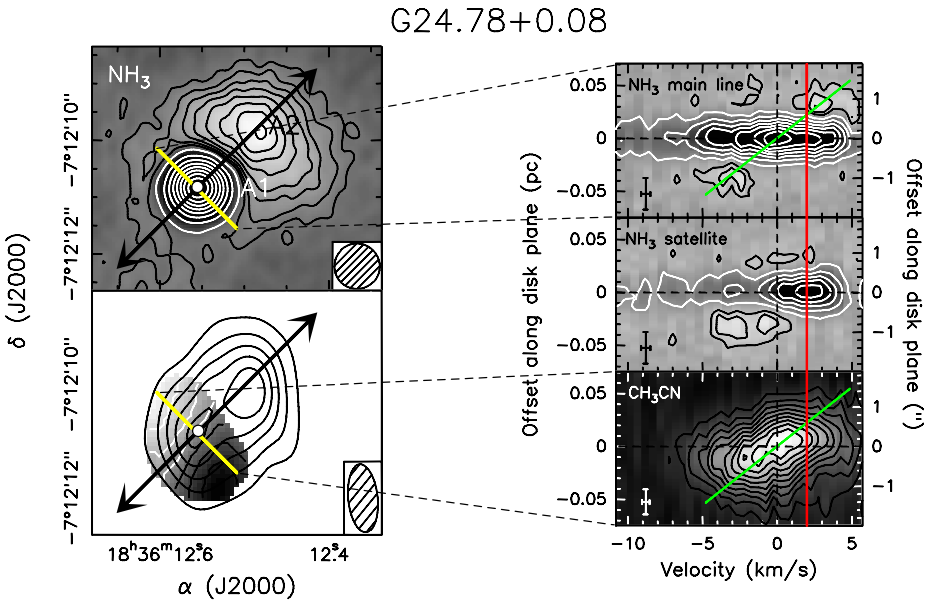

Figure 3. (*Left panels*) Absorption and emission by a molecular gas towards the hypercompact HII region G24 A1. (*Right panels*). Velocity field in the massive toroid G24 A1. See Sect. 3 for details. Figure adapted from Beltrán et al. (2006).

indicate absorption. The black arrows outline the direction of the bipolar outflow (Furuya et al. 2002), ejected along the axis of the toroid. The plane of the toroid is denoted by the line. Note the deep absorption towards the HC HII region (white filled circle) at the center of the toroid. The bottom panel shows the map of the integrated emission of the $CH_3CN(12\text{-}11)$ line (Beltrán et al. 2005) outlining the toroids in G24 A1 and G24 A2. On the other hand, the velocity field of the toroid in G24 A1 is consistent with rotation about the outflow axis. A velocity gradient similar to that in G24 A1, has also been detected in the other core G24 A2 (Beltrán et al. 2004), but is not shown in the figure.

The right panels of Fig. 3 show the position-velocity plots of the $NH_3(2,2)$ main line intensity (*top panel*), the satellite line intensity (*central panel*), and the $CH_3CN(12\text{-}11)K = 3$ line (*bottom panel*) (Beltrán et al. 2006). The positional cut is made along the plane of the toroid P.A.$=-135°$; that is, along the line in the left panels. Both offset and velocity are computed with respect to the star, and the black and white contours correspond respectively to emission and absorption. As can be seen in the central right panel, towards the HC HII region, the satellite absorption is strongly biased towards positive velocities; the peak of the satellite absorption is red-shifted 2 km s^{-1} with respect to the velocity of the star, which is ~ 110.8 km s^{-1}. This can be seen in the $NH_3(2,2)$ main and satellite absorption lines as well, which show the absorption peak clearly red-shifted. The NH_3 main line is seen in absorption at both positive and negative velocities, but the blue-shifted absorption is fainter, broader and more optically thin than the red-shifted one. This is probably due to the gas in the blue-

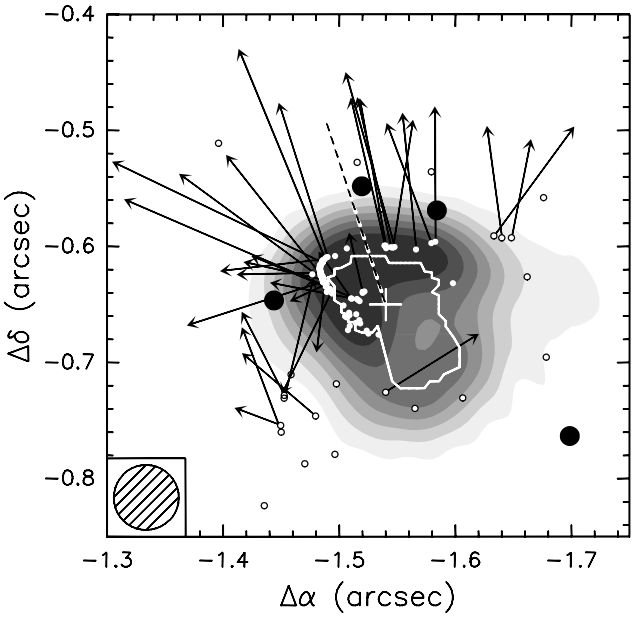

Figure 4. 7 mm continuum image of the hypercompact HII region G24 A1 (*grey scale*) obtained with the VLA plus Pie Town link (Beltrán et al. 2007). The white and black circles denote water and methanol maser spots observed with the VLBA and EVN, respectively (Moscadelli et al. 2007). For some of these spots, proper motions between 20 and 80 $\mathrm{km\,s^{-1}}$ (*black arrows*) have been measured. Note how the water masers trace expansion of the HC HII region. The white line connects the peaks of the profiles obtained from a large number of slices trough the barycenter (*white cross*). Figure adapted from Beltrán et al. (2007).

shifted lobe of the molecular outflow. The velocity gradient seen in the CH_3CN line (Beltrán et al. 2004) (indicated by the tilted line in the bottom left panel of Fig. 3) is detected also in the NH_3 main line, as shown by the tilted line across the two emission peaks (*right top panel*), confirming the presence of rotation.

The mass accretion rate, $\dot{M}_{\rm acc}$, derived assuming that the gas is undergoing free-fall infall onto the star in the HII region is $\dot{M}_{\rm acc} \simeq (\Omega/4\pi)\,(4 \times 10^{-4}$–$10^{-2}\ M_\odot\ \mathrm{yr^{-1}})$, for a solid angle Ω. $\dot{M}_{\rm acc}$ has been estimated for a radius of $0.0037 < R < 0.037$ pc, at which the infall velocity of $\sim$2 $\mathrm{km\,s^{-1}}$ is obtained. This accretion rate is much larger than the critical rate above which the formation of an HII region is inhibited (Walmsley et al. 1995) if accretion is spherically symmetric (i.e., for $\Omega = 4\,\pi$). For an O9.5 star this is $\dot{M}_{\rm inh} \simeq 8 \times 10^{-6}\ M_\odot\,\mathrm{yr^{-1}}$, much less than $\dot{M}_{\rm acc}$: this should suffice to prevent the formation of an HII region. The fact that, instead, an HII region is detected can be explained only if the accretion is not spherically symmetric ($\Omega < 4\,\pi$), which in turn supports the existence of a circumstellar disk-like structure, detected by us on a larger scale as a toroid.

4. Expansion of the HC HII region in G24 A1

Recent high-angular resolution observations seem to suggest that direct accretion onto the central massive protostar might have finished. On the one hand, water maser VLBA observations carried out by Moscadelli et al. (2007) have clearly shown evidences for expanding motions perpendicular to the outflow main axis; that is, along the plane of the rotating and infalling toroid. The proper motions of the water maser spots, which have a mean value of ∼40 km s^{-1}, are directed approximately perpendicular to the geometrical distribution of the maser features. In addition, high-angular resolution observations of the continuum emission at 7 mm and 1.3 cm carried out with the VLA in the A configuration plus the Pie Town link, show that the HC HII region, which is resolved at both wavelengths, shows limb-brightening (see Fig. 4), and has an outer radius of ∼550 AU. What is more important, the water maser features are distributed along the border of the ionized gas. Thus, the position and geometry of the continuum source suggests that the motion of the water masers could be driven by the expansion of the ionized gas.

The ring or shell morphology is also visible in the emission profiles obtained at different angles by taking slices passing through the barycenter of the HC HII region. These profiles show two peaks. The ring is quite evident when joining the positions of these peaks, as can be seen in the white line of Fig. 4. This suggests that we are observing an ionized gas shell. The intrinsic diameter of the ring can be derived by fitting the normalized temperature profile along a cut passing through the barycenter and the emission peak at 7 mm. The best fit is obtained for $R_{\rm i}/R_{\rm o} \simeq 0.9$, which indicates that the shell is very thin, and for a radius of the shell of ∼590 AU (Beltrán et al. 2007).

The HC HII region appears to be expanding. However, due to the high velocities measured through the water maser emission (∼40 km s^{-1}), the expansion cannot be caused by the thermal pressure of the ionized gas, at least in the case of constant density. In such a case, one would expect velocities of about 10 km s^{-1}; that is, the sound speed of the ionized gas. Hence, it must be an additional mechanism driving the expansion of the HC HII region. This mechanism could be a powerful stellar wind. Shull (1980) has modeled the expansion of a very thin ionized shell driven by a powerful wind. In Shull's model, there is an initial phase of free expansion at the wind velocity, when the winds sweeps up its own mass in stellar matter, and then, the system evolves into a four-zone structure in which a thin, dense, ionized shell containing most of the swept up material is created (Shull 1980). Two phases can be identified in this process: a pressure-driven expansion followed by a momentum-driven expansion.

Beltrán et al. (2007) have plotted the flux density at 1.3 cm and 7 mm, the radius and the velocity of the expanding shell as a function of time, for a wind mechanical luminosity of 10^{36} ergs and a density of 10^7 cm^{-3}, consistent with the observations, for two different models: a classical HII region, and a wind-driven shell. However, only the wind-driven model can fit all the data and reproduce the corresponding observed values.

It should be noted that the dynamical time scales involved in the expansion of the HC HII region are very short, 21–66 yr. This implies that the size variation expected in only 5 yr (∼10 mas) should be easy to reveal using the water maser spots as probes. In addition, such short time scales also suggest that the

shell expansion could probably be an episodic event, as statistically it is very improbable that we have been able to observe such a unique event.

5. Rotation or expansion?

There is still the possibility that the velocity gradient observed in the thermal CH_3CN line, as well as in the CH_3OH maser emission, is due to expansion rather than to rotation. In such a case, there would be a collimated compact bipolar outflow perpendicular to the outflow seen on a larger scale in the CO(1–0) line. To discard, or confirm, this possibility, we carried out SiO VLA exploratory time observations towards G24 A1. These observations have revealed a jet-like, bipolar outflow oriented in the same direction as the molecular outflow seen in CO. Therefore, this gives support to the interpretation of rotation for the CH_3CN velocity gradient, as stated by Beltrán et al. (2004).

6. G24 A1: the global view

G24 A1 is an O-type star of 20 $M_\odot$ where, *for the first time*, the simultaneous presence of rotation, outflow and infall has been detected towards a massive young stellar object. The large mass accretion rate and the existence of a HC HII region at the center of the rotating toroid confirm that the accretion cannot be spherically symmetric, but must occur in a circumstellar disk-like structure.

High-angular resolution radio continuum and water maser observations indicate that the HC HII region is expanding on a very short time scale. The infalling gas is no longer accreting onto the central star, but it is stopped at the surface of the HC HII region right at the shock front traced by the water maser spots. CH_3OH masers appear to lie further from the HC HII region, may be located in the pre-shock material, and might still be participating in the infall.

The most important conclusion of this work is that even if the accretion phase were finished, the presence of a rotating toroid, infalling on a HC HII region, which is located at the base of a powerful bipolar outflow, is broadly in agreement with the expectations of the non-spherical accretion scenario for the formation of massive stars.

References

Beltrán, M. T., Cesaroni, R., Codella, C., Testi, L., Furuya, R. S., & Olmi, L. 2006, Nature, 443, 427
Beltrán, M. T., Cesaroni, R., Moscadelli, L., & Codella, C. 2007, A&A, L13-L16
Beltrán, M. T., Cesaroni, R., Neri, R., et al. 2005, A&A, 435, 901
Beltrán, M. T., Cesaroni, R., Neri, R., et al. 2004, ApJ, 601, L187
Codella, C., Testi, L., & Cesaroni, R. 1997, A&A, 325, 282
Furuya, R. S., Cesaroni, R., Codella, C. et al. 2002, A&A, 390, L1
Moscadelli, L., Goddi, C., Cesaroni, R., Beltrán, M. T., & Furuya, R. S. 2007, A&A, 472, 867
Shull, J. M. 1980, ApJ, 238, 860
Walmsley, M., Dense cores in molecular clouds, Rev. Mex. Astron. Astrophys. Conf. Ser., 1, 137-148 (1995)